# A Multiport DC Transformer to Enable Flexible Scalable DC as a Service

Mickael J. Mauger, Vikram Roy Chowdhury, Prasad Kandula and Deepak Divan
*Center for Distributed Energy, School of Electrical and Computer Engineering*
*Georgia Institute of Technology, Atlanta, USA*
mickael.mauger@gatech.edu

***Abstract*— The rapid adoption of new DC loads and sources, including photovoltaic arrays, DC fast charging of electric vehicle, battery energy storage and data centers, requires a large amount of DC power conversion. A majority of new deployments also necessitate the integration of multiple DC loads and sources at one site. The traditional approach to serve these new applications relies on multiple standard power converters, each dedicated to a source or load, and results in highly customized systems, with challenging control coordination, complex protection strategies, and poor scalability. Instead, this paper proposes the concept of a multiport DC transformer (MDCT) as a modular building block for realizing a flexible, scalable DC as a Service system and address this rapidly growing need. The MDCT uses the S4T to achieve very tight control of cycle-by-cycle energy exchange between multiple ports, with high efficiency. A single multiport converter replaces 4-6 distinct converters, integrates all energy flows and manages protection. A new layered control architecture is introduced to ensure stability and scalability of the MDCT, with multiple S4T power converter building blocks connected in parallel to realize a fully modular system and reach the target power levels.**

***Keywords— Current Source Inverter, DCaaS, DC as a Service, MDCT, modular power converter, multiport converter, S4T, solid-state transformer, soft-switching, ZVS.***

## I. Introduction

The last few decades have seen explosive growth of new loads and sources that intrinsically consume or generate large amounts of DC power. This includes photovoltaic arrays, battery energy storage, data centers, DC fast charging of electric vehicles, and electrolysis for hydrogen generation. Deployment of these new loads/sources is expected to represent over 90% of new load and to exceed 100's of gigawatts/year, with individual installations reaching 0.1 MW to >100 MW capacity [1]. DC voltages for these applications range from 200 volts to 2000 volts at point of use, with an optimum power rating of around 0.1 MW to 2 MW per replicable modular building block. Increasing the size of individual modules significantly above these levels increases DC side losses [2]. For such systems, an AC grid connection at the medium voltage level (4 - 34 kV) improves scalability.

While the initial deployments have typically been focused on single use cases (e.g. PV, storage or EV charging), a majority of new deployments are looking at integrating multiple DC sources and loads at one site. For instance, PV and storage are now being preferably deployed over pure PV, as together they offer improved grid services and dramatically improve the dispatchability and capacity factor of the PV plants [2]. Similarly, to offset high peak demand of EV fast charging, batteries and PV panels are also being deployed together. Each type of load and source has unique requirements. Some are unipolar in terms of power flow (PV panels), some are bidirectional (batteries), some may need to add reverse power flow at a later point in time (V2G), and others may need galvanic isolation (PV strings, batteries and EVs).

Today, these deployments are all unique and highly customized systems that are designed using available power converters, each dedicated to a specific DC source/load, and which are then connected together to achieve the desired system level functionality, including appropriate control, coordination, protection and thermal management. The system frequently occupies a substantial footprint and requires significant engineering effort and complex commissioning. Operation and maintenance of such a system also requires expertise and servicing – all factors that add to the cost. Fig. 1 shows a typical example of a 20 MW PV plant with integrated energy storage. The PV field and the battery storage system each require a dedicated inverter, step-up transformer, and protection circuity including AC breakers with high fault-current interruption capability and DC fuses. Several such sub-systems are paralleled to reach the target installation power, and tied to the same point of common coupling (PCC) resulting in well-known coordination challenges of the inverters, including complex fault modes. Similar examples can be shown for plants with PV, storage and EV charging.

There is an unprecedented opportunity for electric utilities to offer DC as a Service (DCaaS), providing a safe protected and standard DC port to which any of the loads and sources discussed above can be connected in a simple and seamless manner, freeing up the customer to focus on their core processes and business. EPRI has been working with utilities for several years on such a concept, shown in Fig 2, based on the idea of solid-state transformers feeding into a DC load center, which then serves a multitude of DC loads and sources [3].

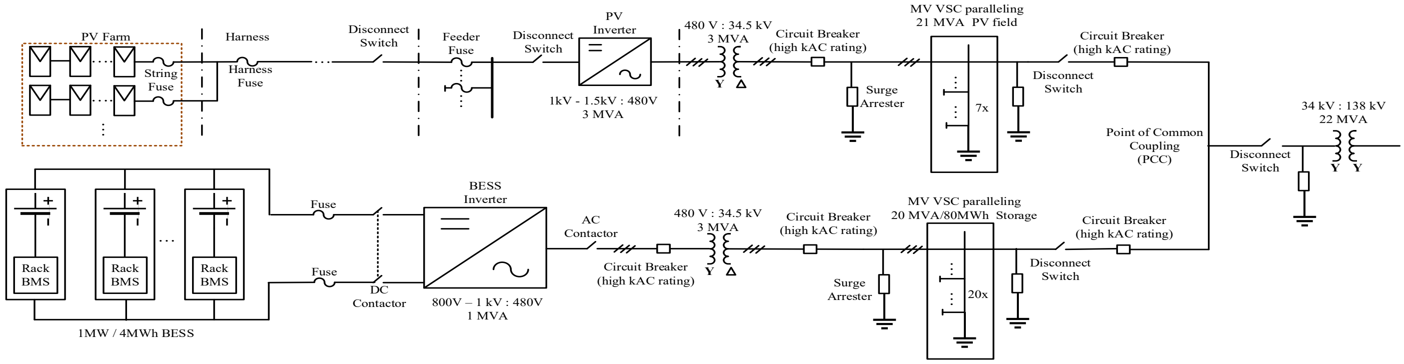


Fig. 1: Example of 20 MW PV plant with energy storage, using dedicated converters for PV and battery integration.

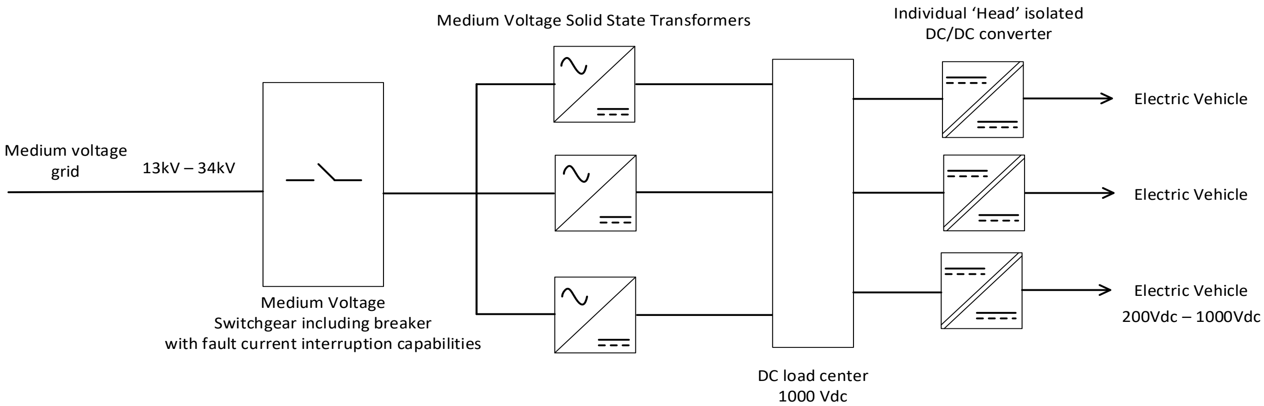


Fig. 2: DCaaS for EV fast charging using medium voltage solid-state transformers and DC load center [3].

Several discrete DC/DC converters are still needed to interface multiple loads/sources and to generate the number of DC ports required. Further, any fault on the common DC bus and load center results in uncontrollable current levels handled through complex and expensive switchgear for protection. Another approach that has been proposed is the use of Medium Voltage String Inverters (MVSI) based on the use of series stacked multiport S4T converters for use in large PV farms with integrated storage [4].

While these approaches are all technically feasible at the converter level, system level implementation raises concerns. Technical solutions for distribution voltages of >13 kV require SiC devices at >3.3 kV, still not economically viable. Issues of managing Basic Insulation Level (BIL) of >90 kV continues to be a challenge, as do issues of transient voltage and EMI management [5]. Finally, AC side fault protection gears, especially on the MV side can be very expensive, particularly if they have to clear high fault currents. As such, none of these approaches seem to realize practical solutions that can be deployed in the near term.

This paper proposes a Multiport DC Transformer (MDCT) that connects directly to medium voltage and serves a as a building block to realize large flexible multiport systems. The rest of the paper is organized as follows. The proposed MDCT approach is presented first, and the multiport operation and topology selection are introduced. The layered control architecture, necessary to the modular system stability, is then detailed. Finally, simulation results are provided to demonstrate the proposed approach.

## II. PROPOSED MULTIPORT DC TRANSFORMER

### A. System Considerations

Looking at the system level implementation, a few things become clear. Standard AC distribution voltages vary over a wide range of 4 kV to 34 kV. As has been seen, managing faults and transients is problematic with MV solid-state transformers, as is the challenge of designing for different line voltages - easily done with a conventional 60 Hz transformer. In addition, 60 Hz transformers can be protected with a simple fusible disconnect at the utility interconnection, providing a low-cost protected interface point with the MV AC grid. Finally, the use of conventional voltage source topologies interconnected through a common DC bus requires multiple DC/DC converters, usually with galvanic isolation, to generate multiple DC connection points. The protection of this DC bus is also challenging and relies on fault interruption capability on both the low-voltage AC and DC sides. Multiple stages of power conversion add complexity and cost, and contribute to system level losses, yet this approach is commonly deployed today.

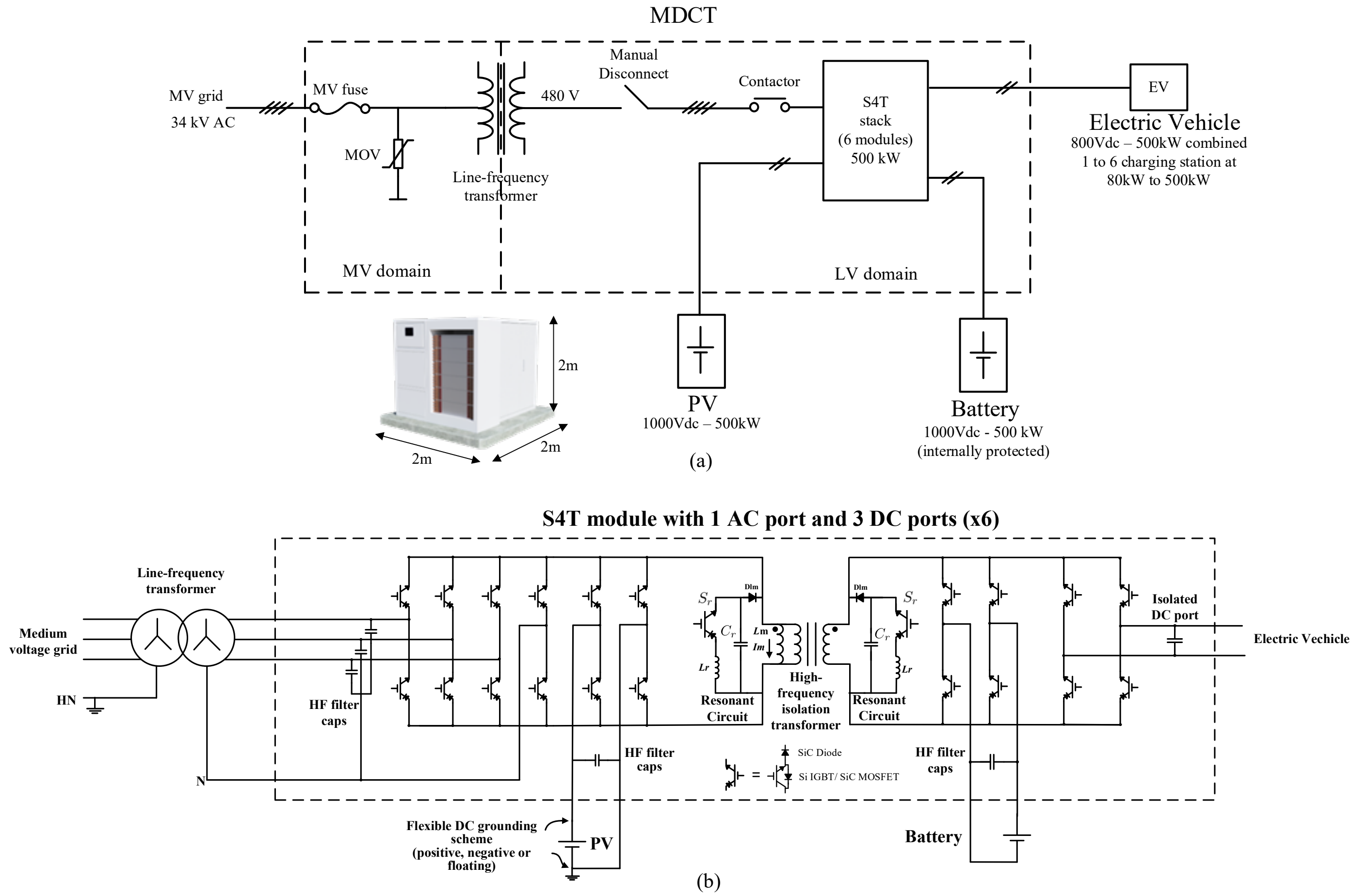


Fig. 3: (a) Single line diagram of possible 500kW implementation of patent pending MDCT connecting to 34kV MV grid and showing multiple DC ports (PV, battery and EV), and device footprint. (b) Detailed S4T module implementation used as building block in MDCT.

In this paper, the authors are proposing a patent pending Multiport DC Transformer (MDCT), based on the integration of a conventional 60 Hz transformer and the single-stage current-source S4T technology, as a building block for flexible and scalable DC as a Service [6]. Fig. 3 shows an implementation for integrating 34 kV MV grid, 1000 Vdc PV panels and batteries, and EV fast charging at 800 volts. Each S4T module is rated at 83.3 kW, for an MDCT system rating of 500 kW. Thanks to the double isolation offered by the 60 Hz transformer and the S4T topology, the PV strings connected to the primary bridge can have a negative ground, preferred for PV arrays, while the battery and EV charging on the secondary bridge can operate with a grounding scheme determined by the vehicle being charged – including the ability to operate with a floating ground. EV charging can be configured flexibly as needed by paralleling the required number of S4T module, for example as six fast chargers at 80 kW each, or two superchargers at 250 kW, or one single truck charger at 500 kW. Currents on all output ports are actively measured and limited, and do not require additional protection gear. DC sources with high short circuit current capacity (e.g., batteries), require internal protection and disconnect, and can safely be directly connected to the MDCT ports. On the input side, any faults in the converter cannot translate into catastrophic faults on the AC side, owing to the current source topology, and can be managed with converter turn-off and contactor in most instances. Faults upstream of the converter, and possibly inside the transformer itself are rare and managed by the input AC side fuse.

The overall footprint is significantly reduced with a fully integrated piece of equipment using fewer components, estimated to ~(2x2x2) meters for a 500 kW MDCT, as shown in Fig. 3, versus ~(10x2x3.5) meters for a similarly-rated system used today [7], a 9X improvement in overall power density. This has big impact on the overall cost of the project, as it reduces electrical, structural, engineering and balance of system costs significantly.

The power electronics in the MDCT is fully modular and based on the S4T topology. The current source nature of the topology, together with the high-frequency isolation, allow for easy paralleling, without issues of circulating currents. This is leveraged in the MDCT by paralleling a number of S4T modules to reach the target system capacity: 6 in this implementation at 500 kW. Each S4T module within the MDCT is configured for multi-port operation and can be interfaced with AC or DC sources as shown in Fig. 3 (b). The number of ports can be extended as needed and at minimum cost, provided the maximum energy transferred over a switching cycle remains bounded [8]. Each port is capable of bi-directional buck-boost operation, and zero-voltage switching of all the main power devices is achieved across the entire voltage and power range thanks to two minimal resonant tank circuits setting the resonant switching transitions. The topology operates at constant switching frequency and is capable of PWM operation, with a simple modulation scheme. A detailed analysis of the principle of operation of the S4T and of the resonant switching transitions can be found in [9]–[13] and is out of the scope of this paper.

### *B. Multiport Operation*

As required for true multiport operation, the power can flow between any numbers of ports from either bridges of the converter, provided the power balance over the switching cycle is met as follows [8]:

$$\sum_{k=1}^{N} I_k V_k = \frac{1}{2} L_m \frac{d}{dt} < i_m^2 > = 0 \qquad (1)$$

where $V_k$ is the equivalent voltage of the k[th] port, $I_k$ is the equivalent current of the k[th] differential port, N is the total number of differential ports, $L_m$ is the magnetizing inductance of the high-frequency transformer, and $<i_m>$ the moving average of the DC-link current in the transformer, over a switching cycle.

A further constraint relates to the DC-link current in the transformer $<i_m>$, which limits the maximum current that can be delivered or sourced to all ports:

$$< i_m > = \frac{1}{1 - D_{lost}} \sum_{k=1}^{N} I_k \qquad (2)$$

with $D_{lost}$ the total duty cycle 'lost' in ZVS transition states and resonance sequence over a switching cycle, kept under 5% in typical designs [10].

In addition to simplifying the system design by realizing the integration and coordination of multiple sources and loads with a single converter stage, the inherent multiport structure of the proposed MDCT also maximizes the utilization of the installed power processing capability. As the same power converter can source and sink power from any number of sources and loads, and the energy dispatch can be adjusted every switching cycle to meet (1), duplicated power conversion infrastructure is eliminated. Taking the example of a 1 MW installation, with 1 MW of PV, 1 MW/ 1 MWh battery storage, 1 MW grid connection, and 1 MW of combined EV charging capabilities, Table I shows the installed power processing capacity for the proposed MDCT approach, and the conventional approach with dedicated power converters for each energy source.

As shown in Table I, the MDCT approach requires 1 MVA of installed power converter capacity, while the standard approach would require 3 MVA of total power converter capacity. The apparent tradeoff with the MDCT approach is that the total power transfer between all energy sources and loads cannot exceed 1 MVA. It is important to note that the MDCT unit can essentially be sized between the maximum power rating of the unitary sources and loads, and the sum of the rated power of the sources and loads (3 MVA in this example). This gives an additional degree of freedom that can be leveraged to optimize system functionality and converter utilization factor.

TABLE I. COMPARISON OF 1MW SYSTEM WITH PV, BATTERY STORAGE, EV CHARGING AND GRID CONNECTION USING STANDARD APPROACH AND PROPOSED MDCT APPROACH.

| Parameter | Standard Approach | MDCT Approach |
|---|---|---|
| Number of converters | 3 | 1 |
| Total installed power converter capcity | 3 MVA | 1 MVA |
| Maximum instantaneous power flow | 3 MVA | 1 MVA |
| Converter utilization factor | Low | Maximum |

### *C. Topology Selection*

The multiport structure of the MDCT is made possible by the S4T topology, which provides a unique single-stage current source converter with high-frequency isolation, soft-switching, and adjustable number of phase-legs to realize the target number of ports of any application. To achieve the same functionality with conventional voltage source converter topologies, a three-stage converter would be required, with a AC/DC front end, a DC/DC high-frequency isolation stage such as a dual-active bridge (DAB) or LLC resonant converter, and a DC/AC back end. Such an approach for a triport configuration using a DAB as isolation stage and interfacing a battery port, a PV port and a three-phase grid port is shown in Fig. 4. The same triport system configuration using the S4T topology is shown in Fig. 5. Assuming a 40 kVA building block, the main design elements, loss estimations, and efficiency projections are given in Table II for the two approaches, as detailed in [8]. Both systems are designed to provide 1.5 pu short-circuit current, inputs and output filters are designed with similar ripple

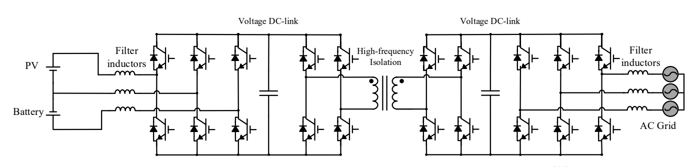


Fig. 4: Isolated triport converter using standard two-level voltage source converter and a DAB stage for isolation.

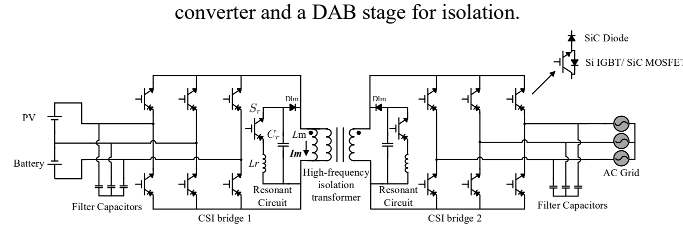


Fig. 5: Isolated triport converter using single-stage S4T topology.

TABLE II
ISOLATED TRIPORT CONVERTER DESIGNS COMPARISON

| Parameter | VSI + DAB – 40 kW (Fig. 4) | S4T – 40 kW (Fig. 5) |
|---|---|---|
| DC-link Voltage/Current | 700 V | 150 A |
| Switch Ratings | 1200 V/150 A | 1200 V/150A |
| No. of Devices | 20 (12 VSI + 8 DAB) | 14 (12 main + 2 ancillary) |
| Conduction Loss (125°C) | 1300 W | 1400 W |
| Switching Frequency | 5 kHz (VSI) – 10 kHz (DAB) | 16 kHz |
| Switching Loss (125°C) | 1000 W (VSI only) | – |
| DC-Link Component | DC Capacitor + HF Transformer | HF Transformer |
| C or Lm value | 2000 $\mu F$ (VSI) + 140 $\mu H$ (DAB) | 350 $\mu H$ |
| DC Stored Energy | 500 J – capacitive | 4 J – inductive |
| AC Filter (10 % ripple) | 4 mH / phase | 90 $\mu F$ / phase |
| AC Filter Stored Energy | 60 J - inductive | 42 J – capacitive |
| Filter / Transformer Losses | 400 W | 250 W |
| Total Losses | 2700 W | 1650 W |
| Full Load Efficiency | 93.3 % | 95.9 % |

specifications and are identical for the AC and DC sides, and the voltage drop across the switch positions is assumed to be the same in both approaches. Owing to their soft-switching operation, the switching losses in the DAB stage and the S4T are assumed to be completely eliminated. More details on the derivations can be found in [8].

As shown in Table II, the single-stage feature of the proposed MDCT using the S4T topology yields significant system-level advantages. The number of semiconductor devices required is reduced and the energy stored in the DC-link and filter elements is minimized, pointing towards a more compact design. The total loss in the VSI based approach is estimated to be 2700 W, while the total dissipation in the S4T-based MDCT is calculated at 1650 W, at full load. This translates into a full-load conversion efficiency of 95.9 % for the S4T-based MDCT, a significant improvement over the full-load efficiency of the VSI-based approach, estimated at 93.3 %. While the use of a current source topology might appear counterintuitive at first glance, the S4T technology is a key enabler of the proposed MDCT approach, with a host of topological and system level benefits over conventional voltage source conversion technologies.

## III. MULTIPORT DC TRANSFORMER CONTROL STRATEGY

### A. *Control Layers*

The MDCT approach follows a modular design and uses several S4T converters as power electronics building blocks connected in parallel to scale in power. The control architecture relies on a layered approach, distributed between the local converter module controllers, and a system controller. The control architecture is shown in the block diagram of Fig. 6.

<u>*Layer 0*</u>: This is the S4T module control layer and is implemented in the converter module local controller. To ensure system stability and scalability with a number of converters connected in parallel, each S4T module port operates as an 'open-loop' current source, using a duty cycle for each port that is computed from the current references provided by the upper layer, and the DC-link current within the module, as follows:

$$D_{port_{k,m}} = \frac{I_{0k,m}^{ref}}{< I_{m,m} >} \tag{3}$$

where, $D_{port_{k,m}}$ is the 'open-loop' duty cycle of the k$^{th}$ port of the m$^{th}$ module, $I_{0k,m}^{ref}$ is the current reference of the k$^{th}$ port of the m$^{th}$ module, and $< I_{m,m} >$ is the average DC-link current of the m$^{th}$ module.

To maintain controllability of the module, the average DC-link current, or transformer magnetization level, must be kept constant. This is achieved in 'Layer 0' with a close-loop control of the DC-link current using local magnetizing current sensing. Under transient conditions, power balance (1) may not be satisfied, and the magnetizing current level might vary widely, especially given that the energy stored in the high-frequency transformer air gap is very small, that is $L_m$ is small. To address this, one of the ports is used as a 'slack bus', where the duty cycle is allowed to deviate from (3). This could be the battery port or the AC grid port. The converter module controller 'Layer 0' uses

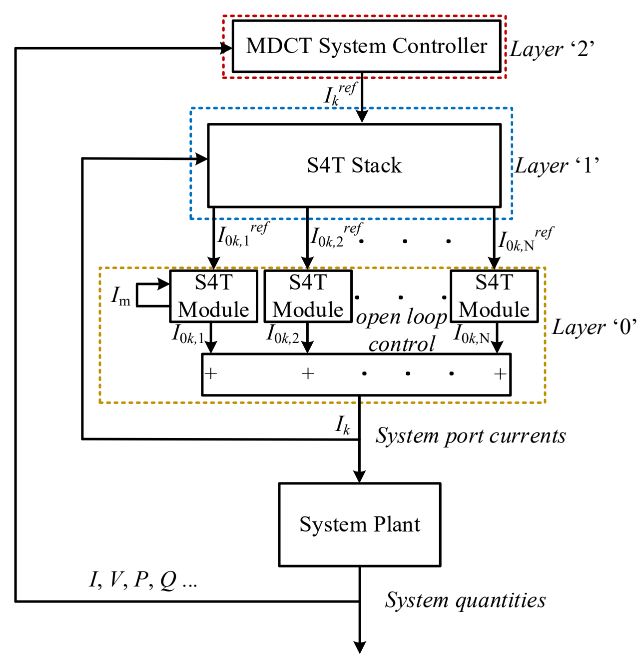


Fig. 6: Flow diagram of the overall MDCT control architecture.

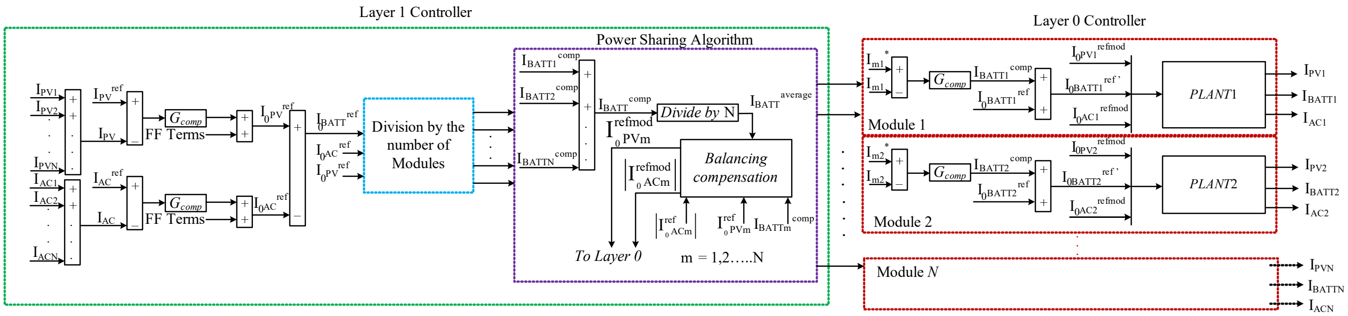


Fig. 7: Simplified block diagram of the overall MDCT control architecture, focusing on the PV, battery and grid port.

this 'slack bus' as a control input, and can compensates for any error in the average DC-link current within a few switching cycles. Given the high switching frequency (≥16 kHz), balance is normally achieved much faster than would be possible with multiple independent power converters that are coordinated using a communication link.

*Layer 1*: This is the control layer at the stack level, where multiple S4T modules are paralleled to reach the target application power. It is implemented in a dedicated stack system controller. This control layer manages the overall power balance within the S4T stack and regulates, in a close loop manner, the currents generated for all system ports, equal to the sum of the currents generated by all modules ports connected in parallel, as shown in Fig. 6:

$$I_k = \sum_{m=1}^{N} I_{0k,m} \tag{4}$$

with $I_k$ the current of the k^th system port, N the number of modules in the stack, and $I_{0k,m}$ the current of the k^th port of the m^th module in the stack.

From the close loop action, 'Layer 1' generates the current references for all ports of all modules in the stack $I_{0k,m}^{ref}$. It also corrects the deviation on the 'slack bus', induced by the control action of 'Layer 0', on a slower time scale, and implements a power sharing mechanism to ensure an even loading of the modules as detailed next.

*Layer 2*: This is the highest control layer, and is implemented in the stack system controller or a plant controller. It is responsible for achieving target control objectives for each system port. A closed loop control is implemented per port on the target control quantity, including system current, voltage, active power or reactive power, etc. This layer in turn generates the current references, for all system ports, to be followed by 'Layer 1'.

A simplified block diagram of 'Layer 1' and 'Layer 0' control architecture is shown in Fig. 7 for an MDCT application in the configuration shown in Fig. 3, and focusing on the battery, PV and grid ports. The architecture follows the layered approach detailed in Fig. 6. By removing any close-loop control actions from 'Layer 0', other than the average transformer magnetization regulation, critical to the converter controllability, the system stability is greatly improved and relies on the passive current-source nature of the topology. The approach also reduces the number of sensors required per S4T module. However, since the close-loop control on the currents of the system ports is implemented at the stack level in 'Layer 1', that is on the aggregated currents resulting from the sum of each S4T module current, it is important to develop a power sharing mechanism to ensure equal loading of all modules in the stack. This is detailed next.

## B. Power Sharing Mechanism

Each S4T module operates in an open-loop fashion on its respective port-currents. Inevitable variability in the power stage, sensing, and control delays of every module would lead to uneven current injection from each converter building block, if identical current references were provided to 'Layer 0' control of all modules. This would in turn lead to uneven power sharing between the modules, and uneven stress on the power electronics. Instead, 'Layer 1' includes a power sharing algorithm as shown in Fig. 7. This power sharing algorithm uses

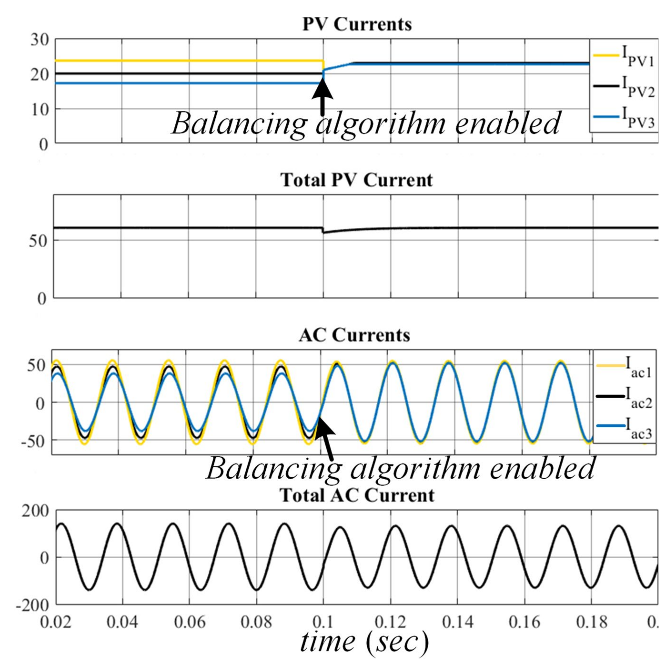


Fig. 8: Simulation results showing the effect of the balancing algorithm.

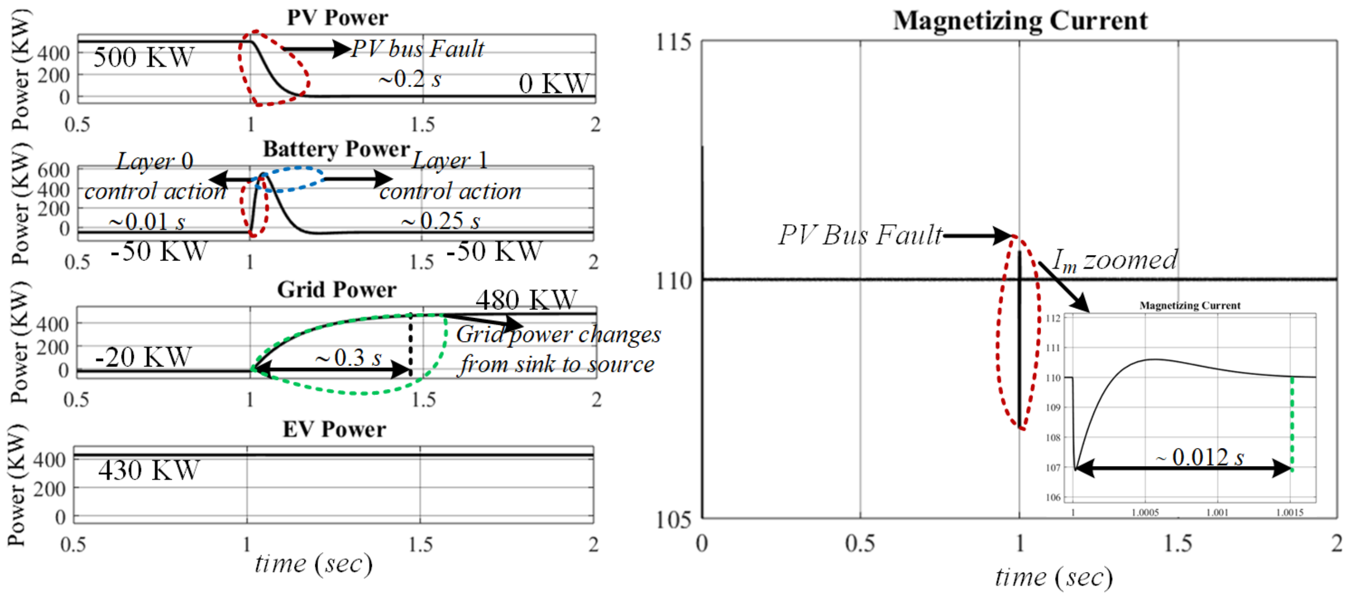


Fig. 9: MDCT power flows and DC-link current under large power transient.

the compensation action of the magnetizing current loops for every ‘Layer 0’ of the modules, ${I_{BATT}}_m^{comp}$, as an observer of current sharing mismatch at the module level. The port current references for the module are then generated for each module, $I_{0PVm}^{refmod}$, $\left|I_{0ACm}^{refmod}\right|$, $I_{0Battm}^{ref}$ in Fig. 7, depending on the estimated power sharing mismatch of the module. The action of the power sharing algorithm thus minimizes the current sharing mismatch between all the modules in the stack, and results in different reference currents being generated for each module. It should be noted that this process does not impact the current delivered at the system port level, thanks to the close-loop action of ‘Layer 1’.

The effectiveness of the power sharing algorithm is confirmed through a simulation study as shown in Fig. 8. In this simulation, the MDCT is controlled to source 68 A of current from the PV array, and 104 Arms from the three-phase grid. Three converter modules are used, and the current per PV port and grid port per module are shown as $I_{PV1}, I_{PV2}, I_{PV3}$ and $I_{AC1}, I_{AC2}, I_{AC3}$, respectively. As seen in the figure, while the system port currents are controlled to their reference value, there is significant unequal current sharing between the three converter modules. This is due to variability in the converter models voluntarily introduced in this simulation to emulate a physical implementation. At t=0.1 s, the power sharing algorithm is enabled, and the current unbalance between the modules is significantly reduced. This leads to a transient error in the system current port, which is corrected in steady-state by the close-loop control action of ‘Layer 1’. It is thus possible to minimize the power sharing unbalance between the converter modules in the stack, without dedicated port current sensing per converter module, and with no impact on the current injections at the system level. Further, the converter modules operate in an open-loop fashion, with the close-loop control for the system ports, and associated sensing, taking place at the system level and in ‘Layer 1’, therefore ensuring the system stability.

This integrated multiport coordination strategy with tiered control layer approach is critical for MDCT operation and is confirmed below through a simulation study.

### C. Simulation Results

In this simulation study, the 500 kW MDCT shown in Fig. 3 is used to charge an electric vehicle at 430 kW (e.g. truck). In this implementation, 6 converter modules are paralleled to reach the target power level. The steady-state power flows for the PV port, the battery port, and the grid port, are 500 kW, -50 kW (battery charging) and -20 kW (injecting power to the grid), respectively as shown in Fig. 9. The MDCT system delivers the target power flows, and the magnetizing current, or DC-link current, per converter module is controlled to the reference value of 110 A.

At t=1 s, a fault is initiated on the PV source, resulting in complete loss of power on the port, and a large transient power unbalance on the system. Within each S4T converter module, control ‘Layer 0’ takes action to restore the power balance at the module level, drawing power from the designated ‘slack bus’ in the system, the battery in this example. Fig. 9 shows the DC-link current of one of the S4T modules within the stack being quickly controlled back to its reference (110 A) within a few milliseconds, as required by the low inertia of the system. This fast control action results in a large deviation on the battery port power with respect to its reference value of - 50 kW. This deviation is then corrected by the action of control ‘Layer 1’ at the system-level and with a slower dynamic, as evidenced in Fig. 9 by the increase in the power drawn from the grid to compensate for the loss of PV and restore the target system power balance. No instability is observed within the system following the large power transient, and the EV power is kept constant through the simulation, thus validating the MDCT control approach and the multiport operation.

## IV. CONCLUSIONS

This paper has provided a first introduction of the concept of a multiport DC transformer as a modular building block for realizing flexible scalable high-power systems to address a rapidly growing market need. There are several unique attributes that the proposed system realizes. The MDCT uses the S4T to achieve very tight control of cycle-by-cycle energy exchange between multiple ports, with high efficiency. A single multiport converter replaces 4-6 distinct converters, integrates all energy flows and manages protection. These S4T converter modules can be paralleled to realize individual MDCT power levels in the range of 0.5 MW – 2 MW. Multiple MDCTs can also be paralleled to realize larger systems. The MDCT can be procured as a single integrated unit that mounts on a pad and directly connects to the MV grid, and offers as many as eight distinct DC ports, each of which is fully bidirectional and has no unprotected fault modes. There is double galvanic isolation, allowing tremendous flexibility in configuring the DC ports – in this study with PV, batteries and EV charging. The grid-facing port can provide a whole range of grid services including P/Q dispatch, frequency regulation, low-voltage/zero-voltage ride through, and inertial support. With the MDCT, it seems now possible to offer DC as a Service, with fully protected and safe DC ports, that are fully monitored, and communication enabled. At the system level, the MDCT enables multiple value streams and reduces engineering complexity which allows more rapid scaling.

Experimental demonstration of a 300 kW MDCT connected to 13 kV, showing buck-boost voltage control, low harmonics and bidirectional power flow control on multiple DC ports is underway. Operation under various fault modes will also be studied and demonstrated.

## ACKNOWLEDGMENT

This work was carried out at the Center for Distributed Energy, Georgia Institute of Technology. The project was partially funded by the Department of Energy Solar Energy Technology Office under award DE-EE0008351.

## REFERENCES

[1] "Global cumulative installed solar PV capacity 2019," *Statista*. https://www.statista.com/statistics/280220/global-cumulative-installed-solar-pv-capacity/ (accessed Feb. 07, 2021).

[2] Z. An, R. P. Kandula, and D. Divan, "Comparative Investigation of System-Level Optimized Power Conversion System Architectures to Reduce LCOE for Large-Scale PV-Plus-Storage Farms," presented at the 2021 IEEE Energy Conversion Congress and Exposition (ECCE), Oct. 2021.

[3] W. Collins, "DC as-a-Service: DOE and SPN," 2019. Accessed: Jul. 26, 2021. [Online]. Available: https://assets.ctfassets.net/ucu418cgcnau/1KXZOT2rzwjYMa9LxpqZIb/d9178a5829563bdfbfacc09fc8e11560/D2-2_-_March_2019_EPRI_IWC_-_S2_Collins.pdf

[4] Z. An, X. Han, L. Zheng, K. Kandasamy, R. Prasad Kandula, and D. Divan, "Modular Isolated Soft-Switching Medium Voltage String Inverter for Large-Scale PV Farm," in *2020 IEEE Applied Power Electronics Conference and Exposition (APEC)*, Mar. 2020, pp. 1067–1073. doi: 10.1109/APEC39645.2020.9124584.

[5] C. Xu *et al.*, "Lightning Impulse Protection for Grid-connected Solid-state Transformers," in *2020 IEEE Energy Conversion Congress and Exposition (ECCE)*, Oct. 2020, pp. 6057–6064. doi: 10.1109/ECCE44975.2020.9235738.

[6] Mickael J. Mauger, R. Prasad Kandula, and D. M. Divan, "Multiport DC Transformer," Provisional Patent Application filed on 11/10/2020

[7] R. Pollom, "TESLA SUPER CHARGING STATION, MADISON WI." Accessed: Feb. 07, 2021. [Online]. Available: https://www.cityofmadison.com/dpced/planning/documents/3801ewa_site.pdf

[8] D. Divan, R. P. Kandula, and M. J. Mauger, "The Case for Soft Switching in Four-Quadrant Power Converters," *IEEE Journal of Emerging and Selected Topics in Power Electronics*, to be published.

[9] H. Chen and D. Divan, "Soft-Switching Solid-State Transformer (S4T)," *IEEE Transactions on Power Electronics*, vol. 33, no. 4, pp. 2933–2947, Apr. 2018, doi: 10.1109/TPEL.2017.2707581.

[10] M. J. Mauger, P. Kandula, and D. Divan, "Optimal Design of the Resonant Tank of the Soft-Switching Solid-State Transformer," in *2019 IEEE Energy Conversion Congress and Exposition (ECCE)*, Sep. 2019, pp. 6965–6972. doi: 10.1109/ECCE.2019.8912633.

[11] L. Zheng, R. P. Kandula, and D. Divan, "Soft-Switching Solid-State Transformer With Reduced Conduction Loss," *IEEE Transactions on Power Electronics*, vol. 36, no. 5, pp. 5236–5249, May 2021, doi: 10.1109/TPEL.2020.3030795.

[12] H. Chen and D. M. Divan, "Soft switching solid state transformers and converters," WO2017201209A1, Nov. 23, 2017 Accessed: Apr. 30, 2020. [Online]. Available: https://patents.google.com/patent/WO2017201209A1/en

[13] L. Zheng, D. M. Divan, R. P. Kandula, and K. Kandasamy, "Transformers, converters, and improvements to the same," WO2020023471A1, Jan. 30, 2020 Accessed: Jul. 13, 2020. [Online]. Available: https://patents.google.com/patent/WO2020023471A1/en